National Radio Astronomy Observatory
Electronics Division Technical Note
EDTN #231

Design of a Rectangular to Circular Waveguide Transition for ngVLA Band 3

B. DuVerneay, R. Lehmensiek, W. Grammer (NRAO)

February 13, 2025

Introduction

Orthomode transducers (OMTs) and feed horn antennas often have a circular waveguide port, which supports two linear orthogonal TE_{11} modes. A rectangular to circular transition is an adapter that allows for low-reflection, low-loss transmission between the TE_{10} mode on rectangular port and a TE_{11} mode on the circular port. The transition enables the interface between the test equipment and the device under test.

This memo documents an effort to design a rectangular to circular waveguide transition for the next generation Very Large Array (ngVLA) Band 3 receiver (12.3 – 20.5 GHz). This band uses custom waveguide sizes and does not have off-the-shelf component availability. Existing rectangular to circular transitions for other waveguide sizes appear to have unique geometry definitions. The simulations performed attempt to compare some possible geometries and select the best performing option.

Linear Transition Modeling

Initial Linear Mechanical Models and HFSS simulations

Initially, two methods were used to generate a linear transition from rectangular WR-56.3 (0.563” x 0.2815”, or 14.3 mm x 7.15 mm) to circular (17.08 mm diameter) waveguide:

1) Using Autodesk Inventor software, sketch a rectangle and circle separated by the transition length, then use the Loft command to create a 3D solid. The Loft command options are set to the defaults. This will be referred to as “Model 1.”

2) Using TICRA Tools CHAMP 3D software, generate a linear transition of a specified length. A STEP file of the model is exported from the software. This will be referred to as "Model 2."

10 cm long transition models are shown in Figure 1. It is apparent from the image that the models are not equivalent - the edges along the length are clearly different.

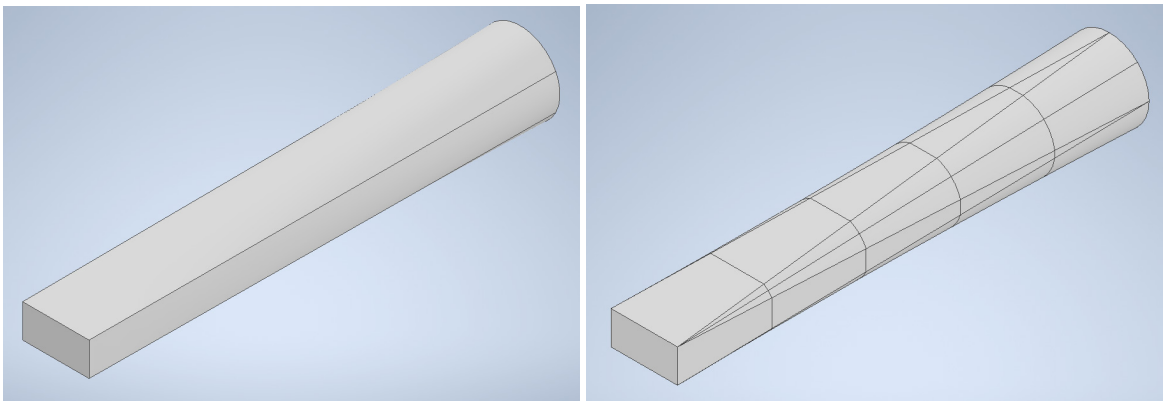

Figure 1. Initial 10 cm Transition Models. Left: Loft (default) in Autodesk Inventor. Right: Generated by CHAMP 3D.

Geometries comparable to both models have been found in existing waveguide transitions. For instance, a WR-22 NRAO transition model for EVLA is similar to Model 1, while a commercially available WR-187 transition resembling Model 2 was found in the Socorro lab.

Next, the mechanical models were imported into Ansys HFSS version 2024R2 and a simulation was set up as follows:

- Mesh: Frequency of 20.5 GHz, Max Delta S = 0.0005, Curvilinear meshing
- Sweep: 12.3 – 20.5 GHz, 0.1 GHz discrete steps
- Excitations: Port 1 is the circular port, Port 2 is the rectangular port.
- Materials: Vacuum filled waveguide surrounded by boundary walls of pure copper at room ambient ($\sigma = 5.8 \times 10^7$ S/m). No surface roughness was added.
- 1 cm length of circular and rectangular straight waveguide is added to the transition model

Note that 5 modes can propagate in the circular waveguide over the frequency band. The 6th mode has a cutoff frequency (f_c) of 21.41 GHz, which is above the band edge of 20.5 GHz. The modes and cutoff frequencies are listed in Table 1. Orthogonal TE_{11} modes 1 and 2 are the intended modes for propagation of signals in the receiver front-end. A circular waveguide simulation was run in HFSS, and the results agreed well with theory.

Table 1. 17.08mm diameter circular waveguide modes

HFSS Port Mode	Mode Name	f_c
1	TE_{11a}	10.29 GHz
2	TE_{11b}	10.29 GHz
3	TM_{01}	13.44 GHz
4	TE_{21a}	17.06 GHz
5	TE_{21b}	17.06 GHz

Initially, two modes on Port 1 and one mode on Port 2 was simulated in the full physical model for each transition. Additionally, E-plane and H-plane symmetry models were created. These are shown in Figure 2 for the Model 2, CHAMP 3D generated transition.

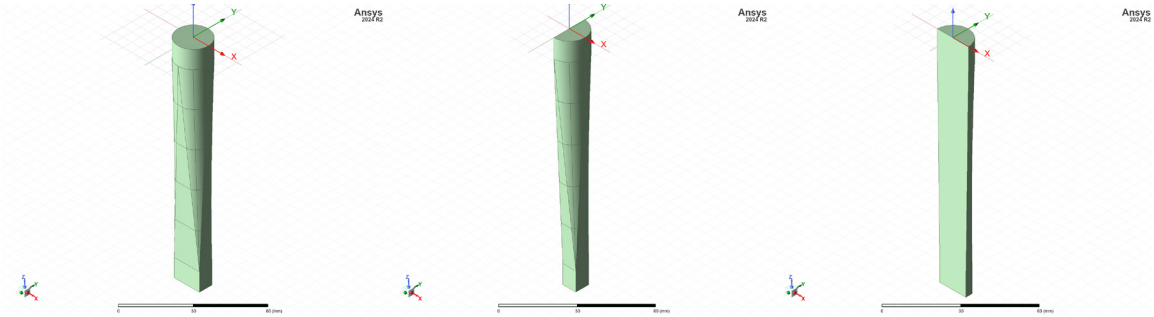

Figure 2. HFSS models for CHAMP 3D transition. Left: No symmetry. Center: H-plane symmetry. Right: E-plane symmetry.

The simulated return loss S(2,2) and transmission S(2,1:1) are shown in Figure 3 and Figure 4, respectively. These initial results indicate that the CHAMP 3D generated model has better return loss at the low end of the band compared to the Inventor model constructed using the default Loft between the circular and rectangular port. Symmetry in the models results in reduction of simulation time and good correlation of results, but does not allow for the simulation of the 2nd degenerate TE_{11} mode and cross-polarization.

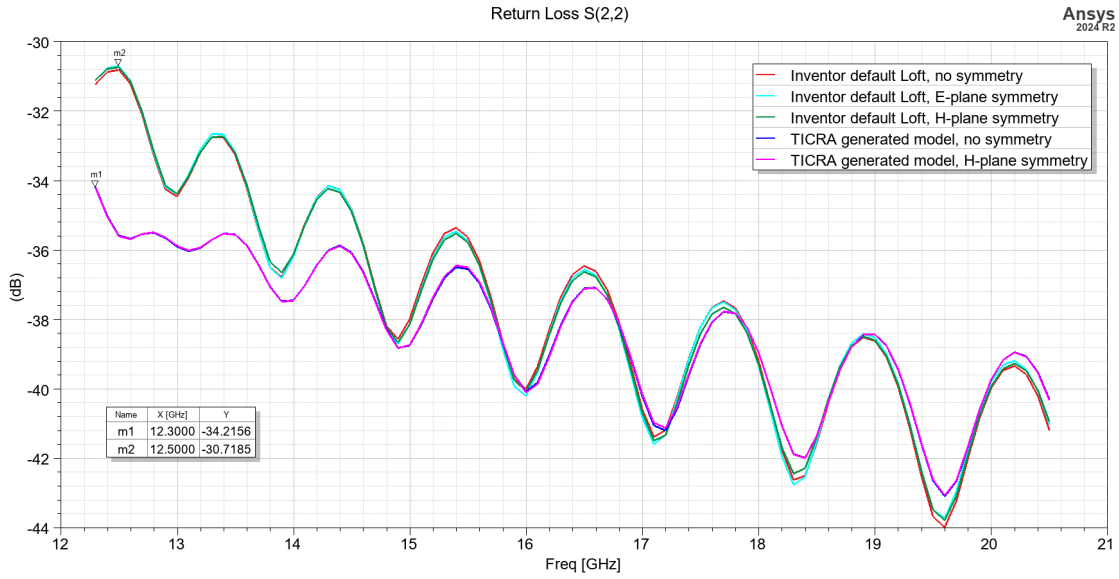

Figure 3. Return Loss of 10 cm length linear transitions

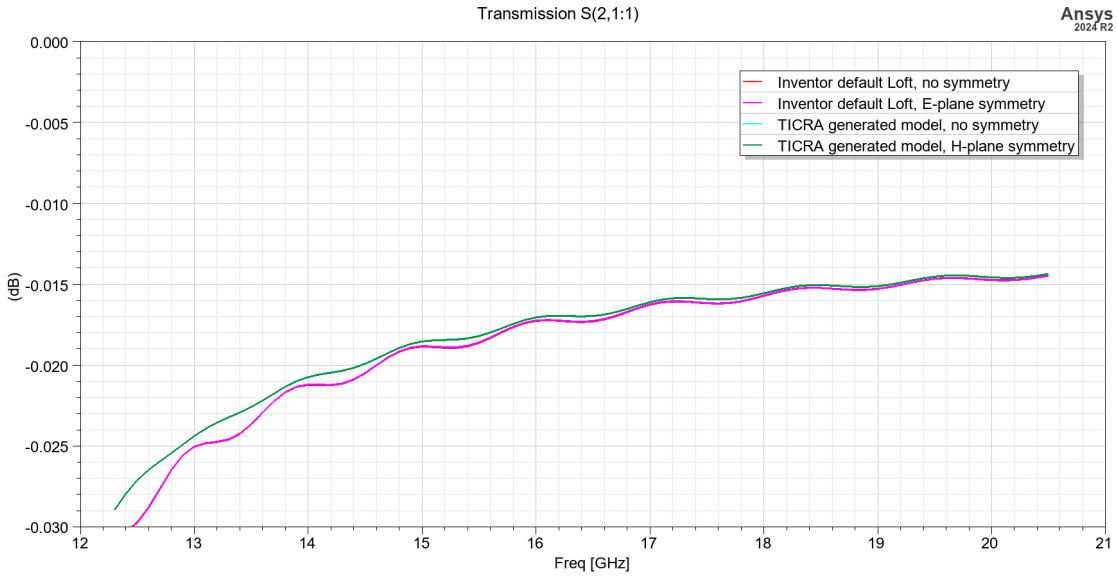

Figure 4. Transmission of 10 cm length linear transitions

The cross-polarization responses S(2,1:2) are plotted in Figure 5. The CHAMP 3D generated model had superior cross-pol performance; however, these results should be taken with some caution. The cross-coupling in each case is quite low and the simulation may have artifacts due to model importing, meshing, or port alignments that could affect the accuracy of the results.

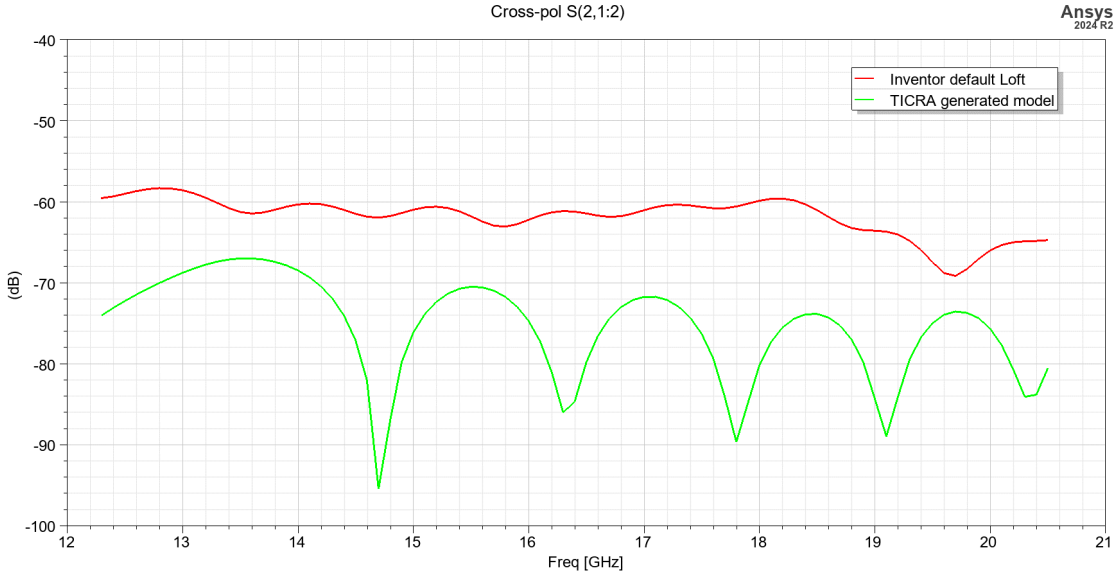

Figure 5. Cross-pol transmission of 10 cm length linear transitions

Additional Linear Models and HFSS simulations

Since the CHAMP 3D exported model had superior performance, attempts were made to model a similar transition in Inventor using 2 techniques:

1) A truncated, right circular cone is constructed by Lofting between two circles separated by the length of the transition, with a starting diameter of the circular waveguide 17.08 mm and the ending diameter of 15.99 mm, sized to circumscribe the WR-56.3 waveguide (calculated as $\sqrt{14.3^2 + 7.15^2}$). Next, four planes are defined using three points each: two vertices from an edge on the rectangle, and one point on the circle at either 0, 90, 180, or 270 degrees. Finally, the material outside of the planes is Split (deleted). The 3 step process used to generate this "Model 3" transition is shown in Figure 6.

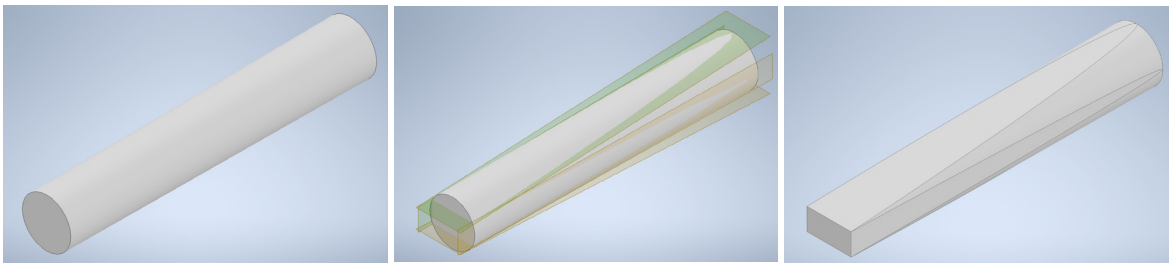

Figure 6. Inventor "Model 3" creation steps. Left: Loft. Center: Define planes. Right: Split.

2) Construct the 4 intermediate cross-sections on work planes along the transition, with dimensions defined in the CHAMP 3D exported model. Loft between these 6 sketches. Note that each intermediate sketch is composed of 4 straight lines and 4 arcs. This completed "Model 4" is shown in Figure 7.

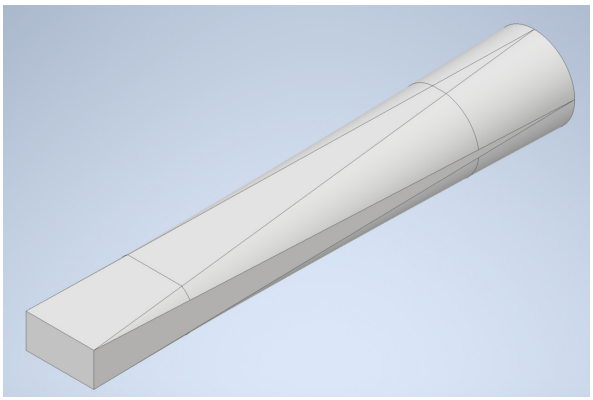

Figure 7. Inventor "Model 4" - Loft between 4 intermediate sketches

Now, there are 4 mechanical models, which are identified as follows:

1) Model 1: In Inventor, Loft between a circle and rectangle, using default settings.
2) Model 2: TICRA Tools CHAMP 3D generated model.
3) Model 3: In Inventor, Loft between a 17.08mm circle to 15.99mm circle, followed by removal of material outside 4 defined planes.
4) Model 4: In Inventor, define the rectangle, circle, and 4 intermediate sketches. Loft between the 6 sketches.

The cross-sections of the 4 models are shown in Figure 8 at 20%, 40%, 60% and 80% along the length of the transition. At each cross-section, Model 1 is composed of 4 arcs. Models 3 and 4 are composed of 4 straight lines and 4 arcs. The CHAMP 3D generated Model 2 actually contains 4 additional vertices and a total of 8 arcs. Model 4 is very close to Model 2, with identical straight lines but only 4 arcs defined, making it a more straightforward geometry to model in comparison.

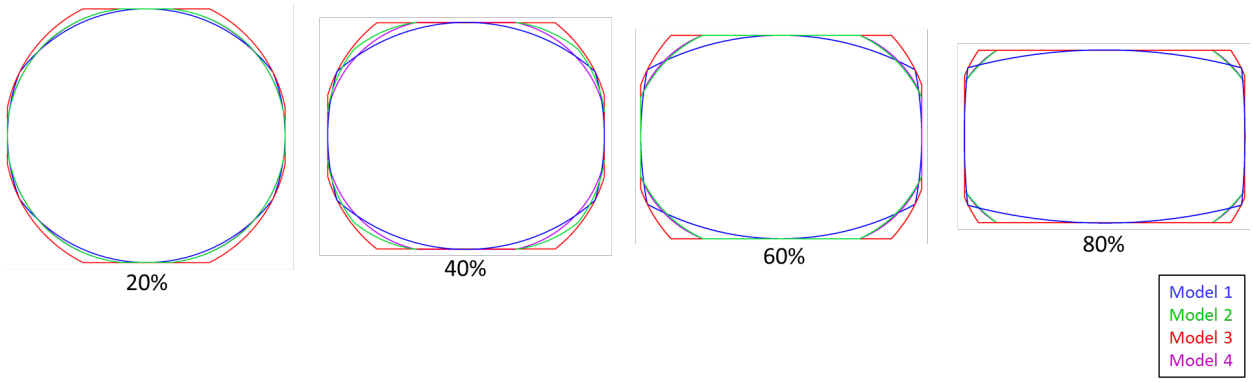

Figure 8. Cross-section comparison along the transition at 20%, 40%, 60% and 80%

HFSS models were constructed for each mechanical model with similar simulation setup as used previously. A comparison of the return loss is shown in Figure 9.

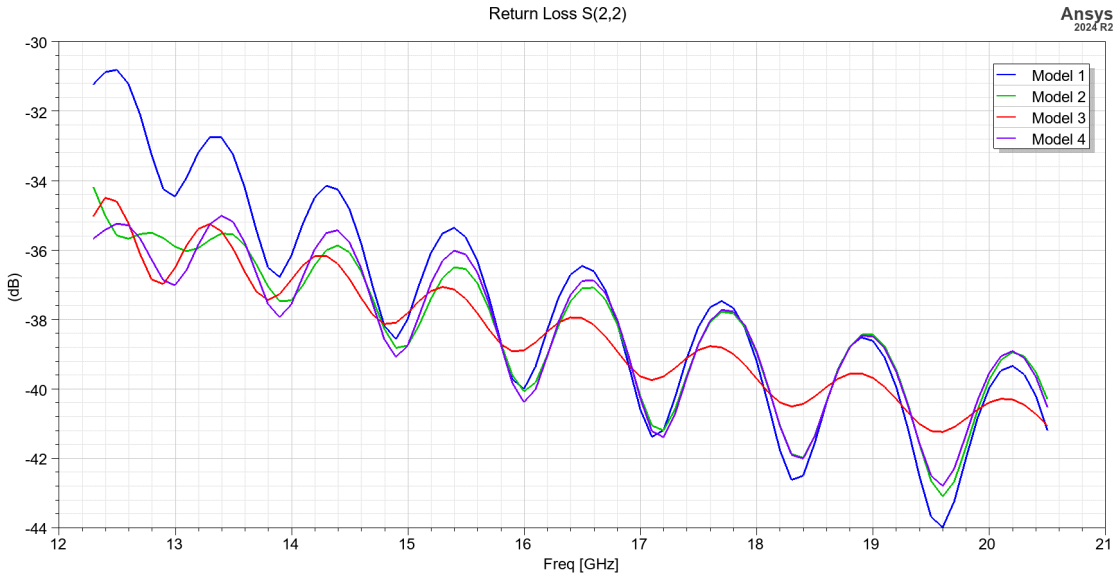

Figure 9. Return Loss Comparison of Models 1-4

In this return loss figure:

1) Model 1, generated using the default Loft in Inventor, continues to be the worst performing transition.
2) Models 2 and 4 have quite similar results, with some deviation at the low end of the frequency band.

3) *Model 3 appears to be the best*. Over the frequency band, the ripple in the return loss is smaller compared to Model 2 and 4. Model 3 has the benefit that it is straightforward to define and model.

Cross-pol results are shown in Figure 10. All models have low cross-pol but the simulation indicates that Model 3 is the best. As noted previously, the relative cross-pol results at these low levels may be in the numerical noise.

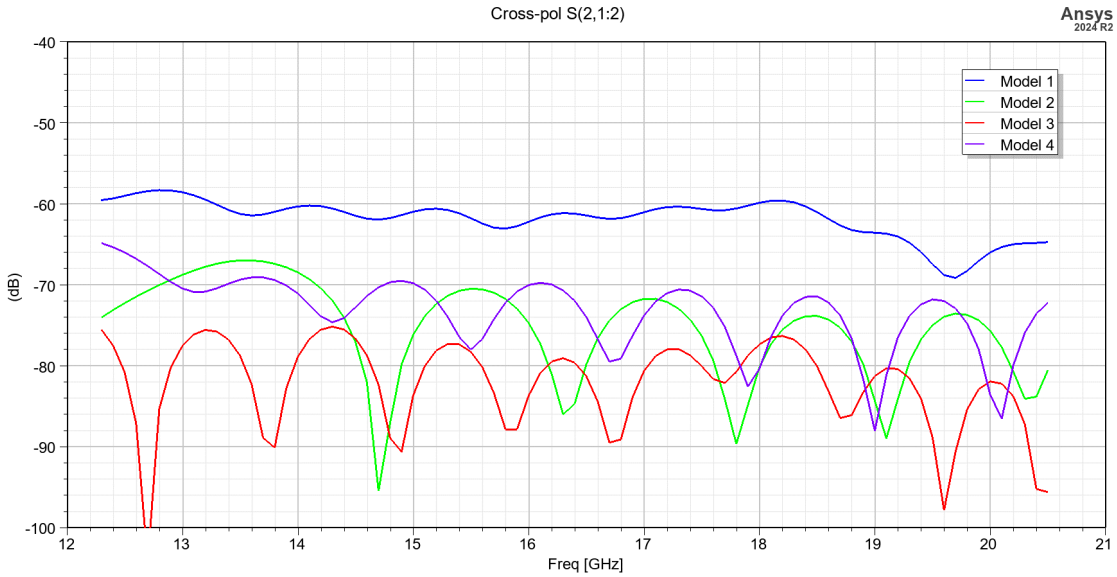

Figure 10. Cross-pol Comparison of Models 1-4

Additionally, the Altair FEKO version 2024 electromagnetic simulation software package was also used to simulate the same transitions, for comparison and validation of the results in HFSS. The return loss and cross-pol are shown in Figure 11 and Figure 12, respectively. There is very good agreement in the return loss responses. The cross-pol responses in FEKO do not align precisely with HFSS, but the simulated magnitude is greater than 60 dB down for all models.

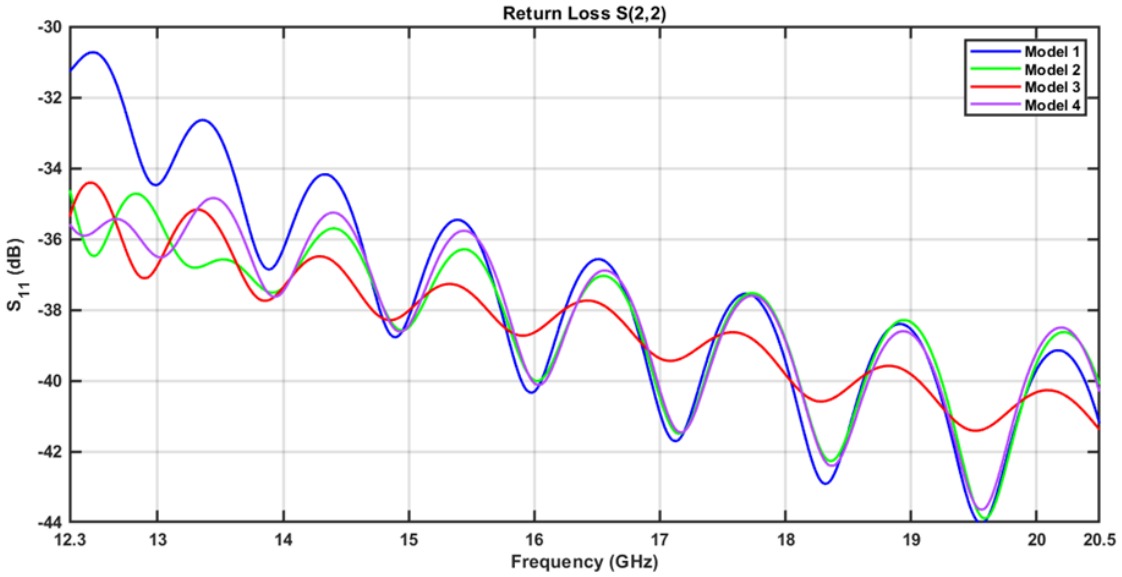

Figure 11. Return Loss Comparison of Models 1-4 (simulated using FEKO software)

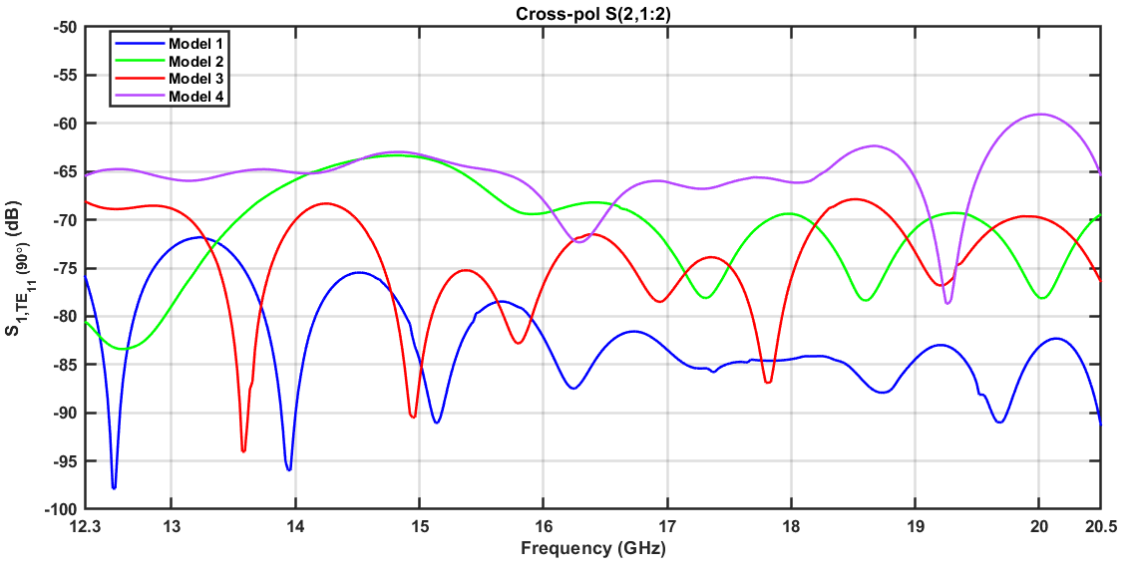

Figure 12. Cross-pol Comparison of Models 1-4 (simulated using FEKO software)

Swept Transition Length

Based on the results, Model 3 is selected as the geometry of choice with a worst case 34.5 dB return loss and 75 dB cross-pol according to the HFSS simulation. However, further improvement in the return loss of the transition may be advantageous, as the feed horn and OMT devices under test are expected to have low losses. Thus, the Model 3 geometry is swept in length from 10 to 18 cm in 2 cm steps. The return loss and transmission results are shown in Figure 13 and Figure 14 respectively. With each step,

an improvement of return loss is achieved. As the length is increased, there are diminishing returns in return loss improvement. The first step in length from 10 cm to 12 cm appears to have the biggest benefit, improving the worst-case return loss to 36.2 dB (VSWR of ~ 1.03), while only adding a very small increase in insertion loss. The contribution of this device to uncertainty in a Vector Network Analyzer correction should be quite low, compared to the coaxial to waveguide adapter that will be required in the path.

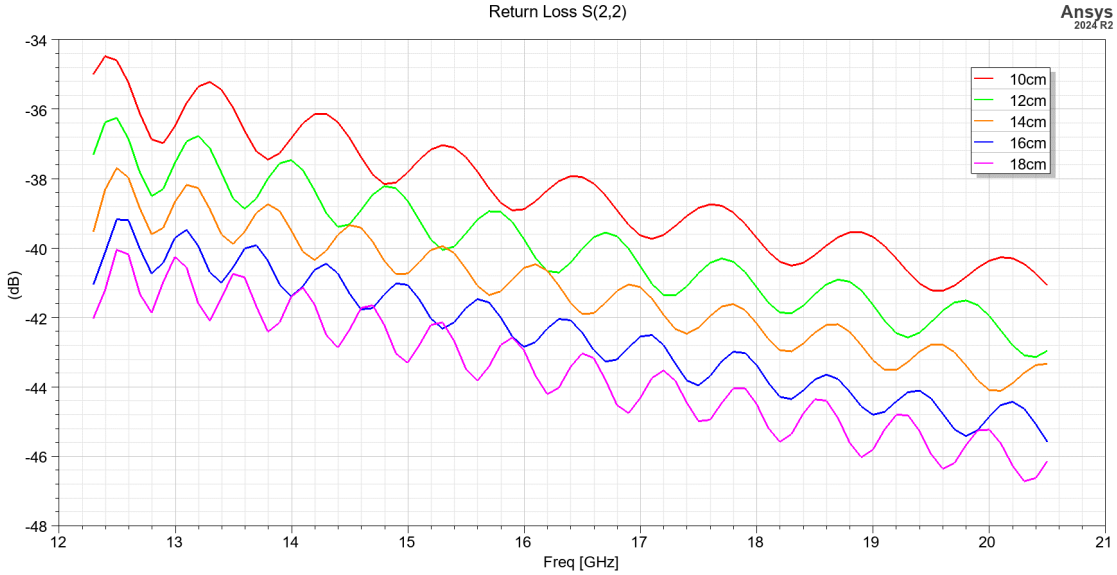

Figure 13. Return Loss – Swept transition length of Model 3 design

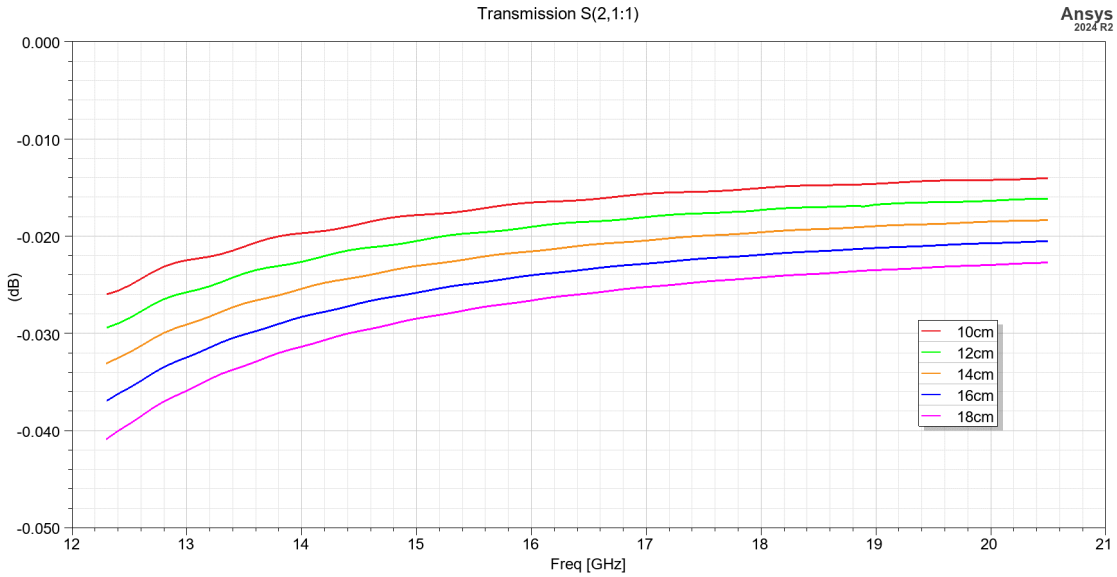

Figure 14. Transmission – Swept transition length of Model 3 design

12 cm length transition - 5 mode circular port simulation

The previous simulations set two modes on the circular port, and symmetry in the model when possible to save simulation time. In this simulation, 5 port modes are simulated on the circular port of the model with no symmetry, as an additional check to validate performance of the 12 cm long transition.

The return loss for each mode and port are shown in Figure 15. The reflection for Modes 1 and 2 at port 1 and the single mode at Port 2 are the same in the simulation, and these results have a good match to the previous simulation with fewer modes. The higher order modes 3, 4, and 5 on port 1 are highly reflected above the cutoff frequency of the mode.

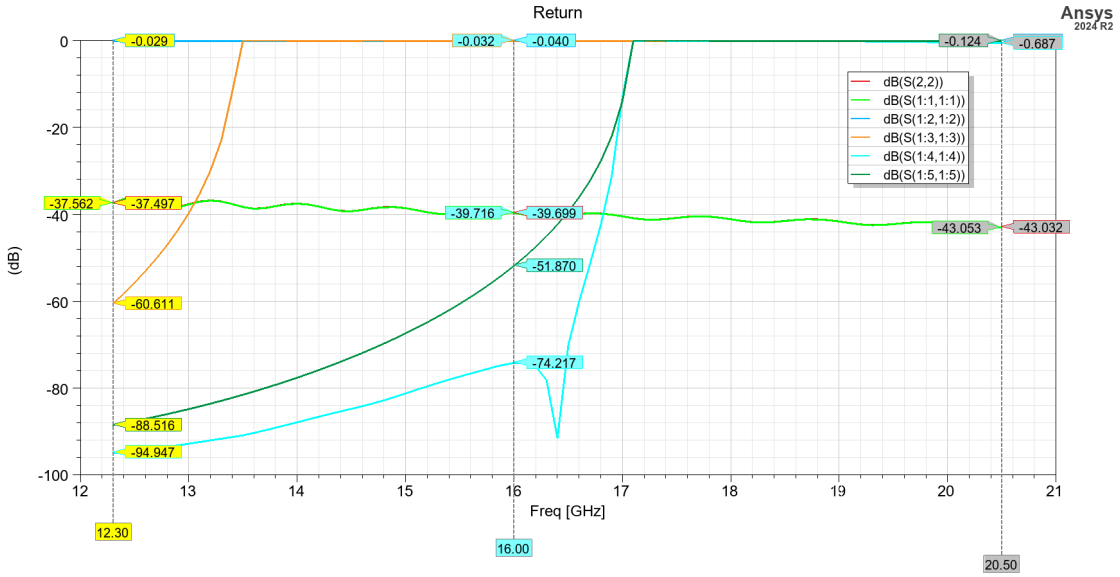

Figure 15. Return Losses simulated for each mode on both ports

In Figure 16, the reflection of each mode with stimulus of the dominant TE_{11} mode is plotted. This shows that the higher-order mode magnitudes are significantly less than the dominant mode and the effect on calibration should be negligible.

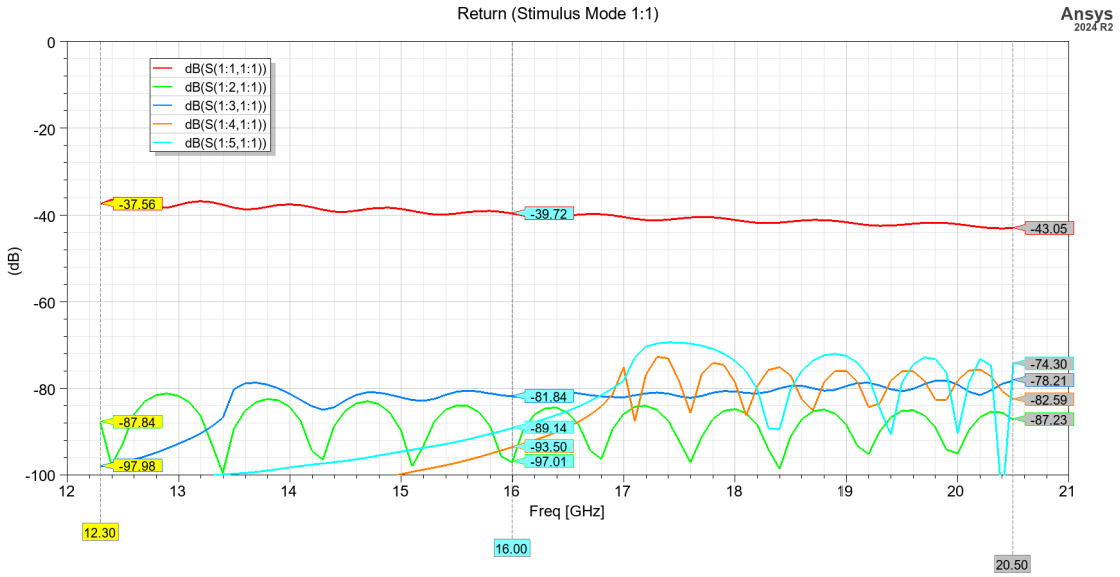

Figure 16. Return Losses simulated for each mode with stimulus of Mode 1 on circular port

The transmission of each mode from Port 1 to Port 2 is shown in Figure 17. These results show that the desired mode is transmitted with low loss across the entire band, while the other orthogonal mode and higher order modes have very low transmission.

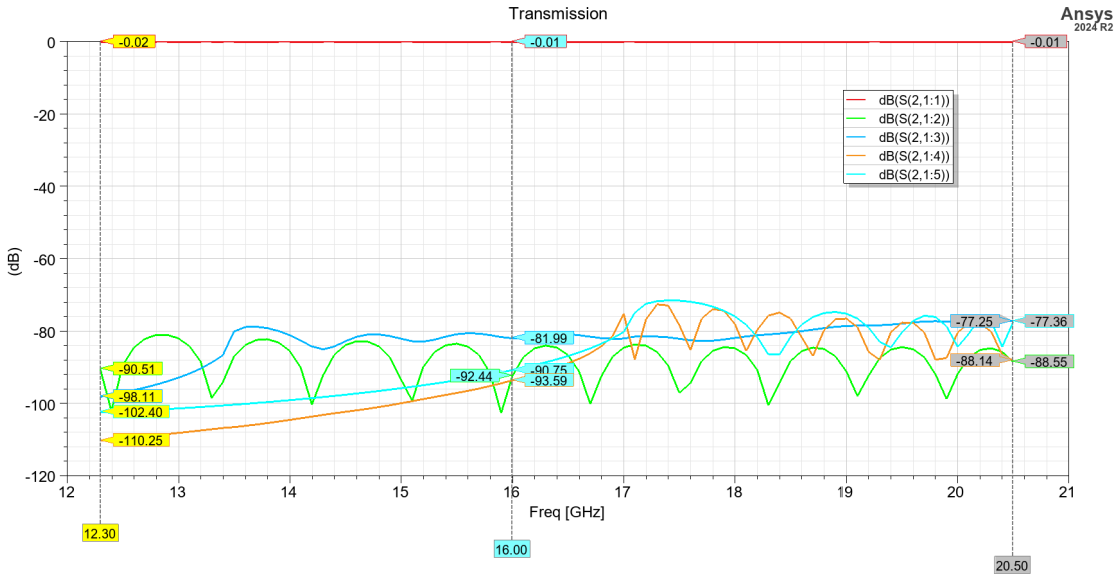

Figure 17. Transmissions for each mode with stimulus on rectangular port

Asymmetry

The previous simulations assumed perfect symmetry in the model. Due to tolerances in manufacturing, the fabricated device will have some asymmetries. The geometry was modified in Inventor as follows to introduce these imperfections, with the truncated cone in the model left unmodified (perfectly fabricated).

1) x-axis offset models: Shift the left and right cutting planes by 0.5, 1, 2, and 5 mils in the same direction. The top and bottom cutting planes are not changed.
2) y-axis offset models: Shift the top and bottom cutting planes by 0.5, 1, 2, and 5 mil in the same direction. The left and right cutting planes are not changed.

The x-axis is defined as being parallel to the broad-wall and the y-axis is parallel to the narrow-wall of the rectangular waveguide cross-section. The x-axis offset models are shown in Figure 18 and Figure 19 from 2 different perspectives.

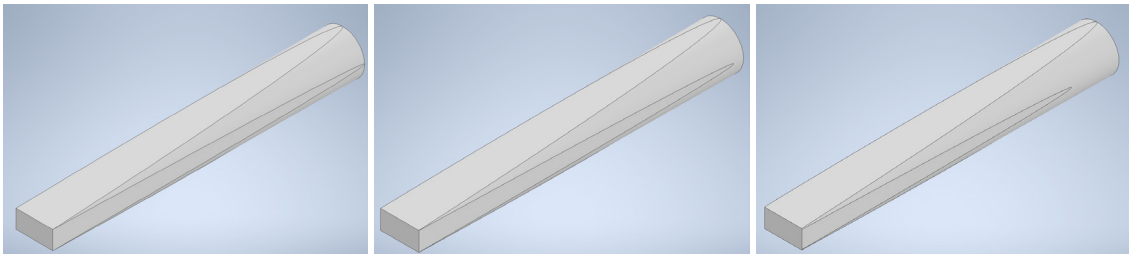

Figure 18. x-axis offset models from perspective 1. Left: No offset. Center: 1 mil offset. Right: 5 mil offset.

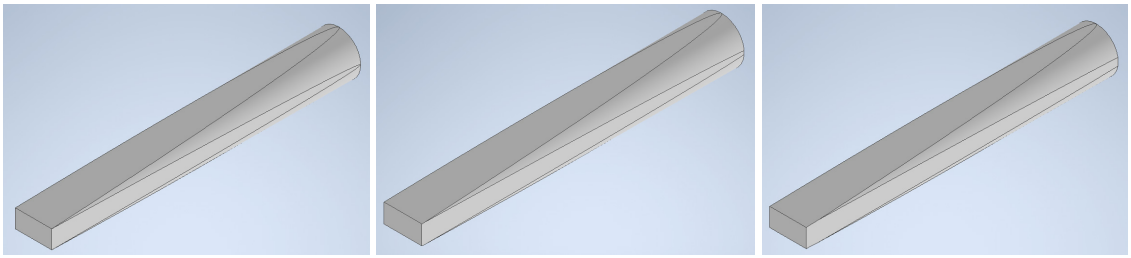

Figure 19. x-axis offset models from perspective 2. Left: No offset. Center: 1 mil offset. Right: 5 mil offset.

The y-axis offset models are shown in Figure 20 and Figure 21.

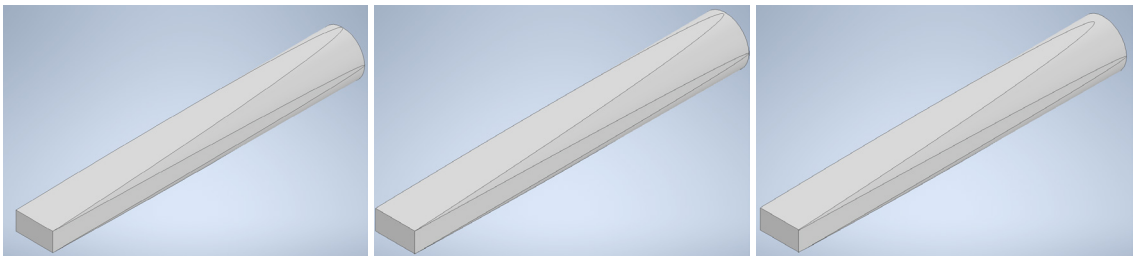

Figure 20. y-axis offset models from perspective 1. Left: No offset. Center: 1 mil offset. Right: 5 mil offset.

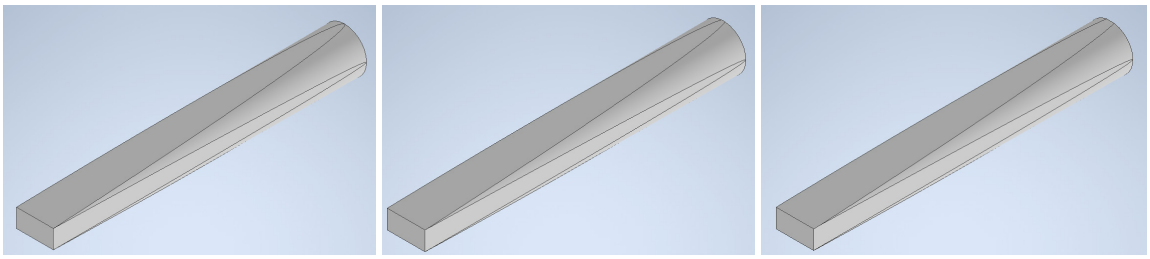

Figure 21. y-axis offset models from perspective 2. Left: No offset. Center: 1 mil offset. Right: 5 mil offset.

A perfect 1 cm section of waveguide was added to the rectangular and circular waveguide ports and then simulated in both HFSS and FEKO. Good correlation in return loss response was observed between the simulators, but cross-pol and higher order mode transmissions had some inconsistencies in how well the results agreed. It is believed that the FEKO results were more reasonable and believable, thus, those results are included in this memo.

The return loss vs. x-axis and y-axis offsets are shown in Figure 22 and Figure 23, respectively. There is little change in the results up to a 1 mil offset. At 5 mil offset there is noticeable degradation in the y-axis offset return loss. The y-axis offset appears to be more sensitive than the x-axis offset.

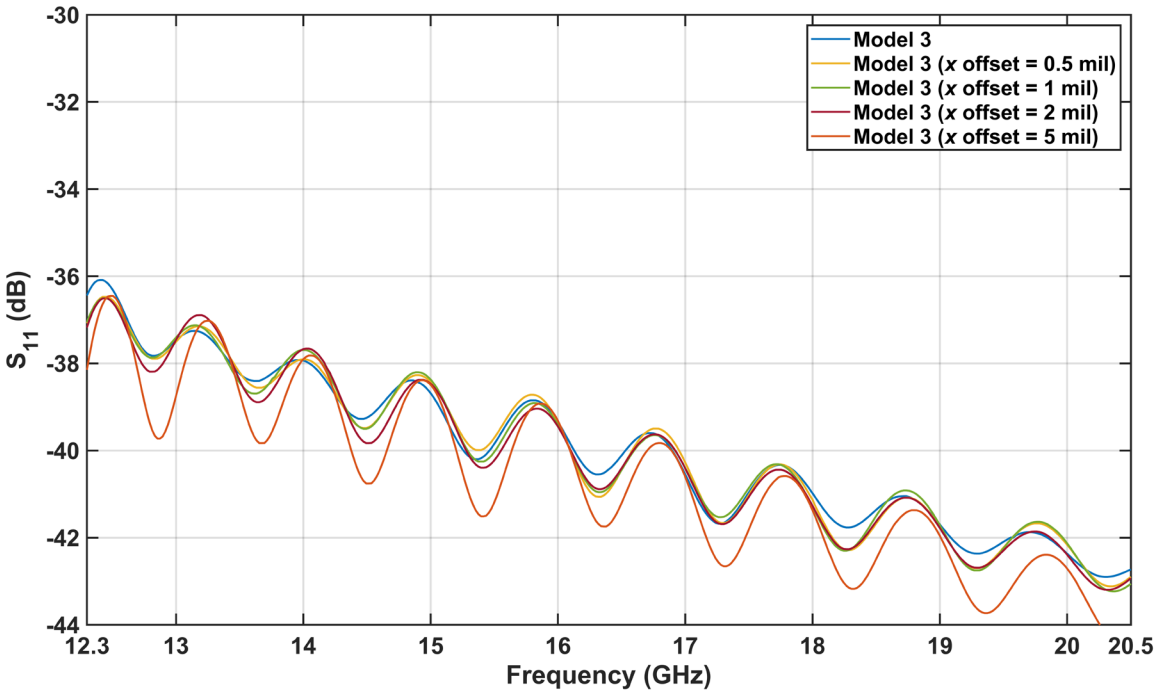

Figure 22. Return Loss vs. Tolerance (offsets in x-axis)

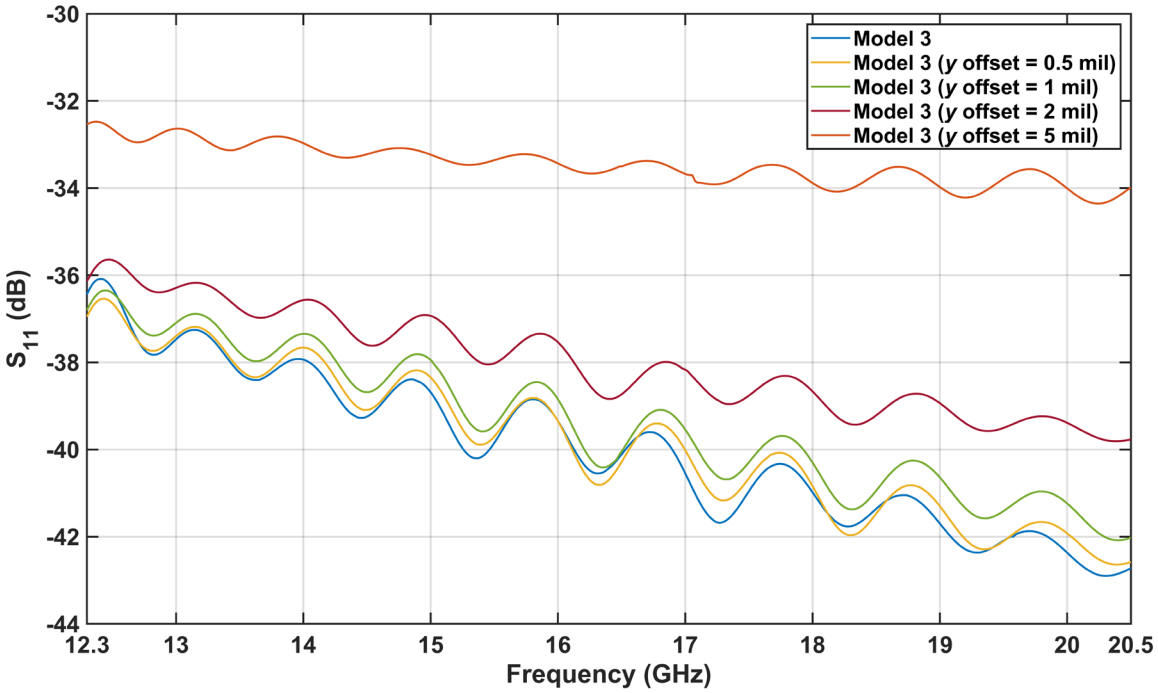

Figure 23. Return Loss vs. Tolerance (offsets in y-axis

The cross-pol vs. x-axis and y-axis offsets are shown in Figure 24 and Figure 25, respectively. Very low cross-coupling is simulated, with no substantial degradation due to tolerance within the numerical noise of the simulation.

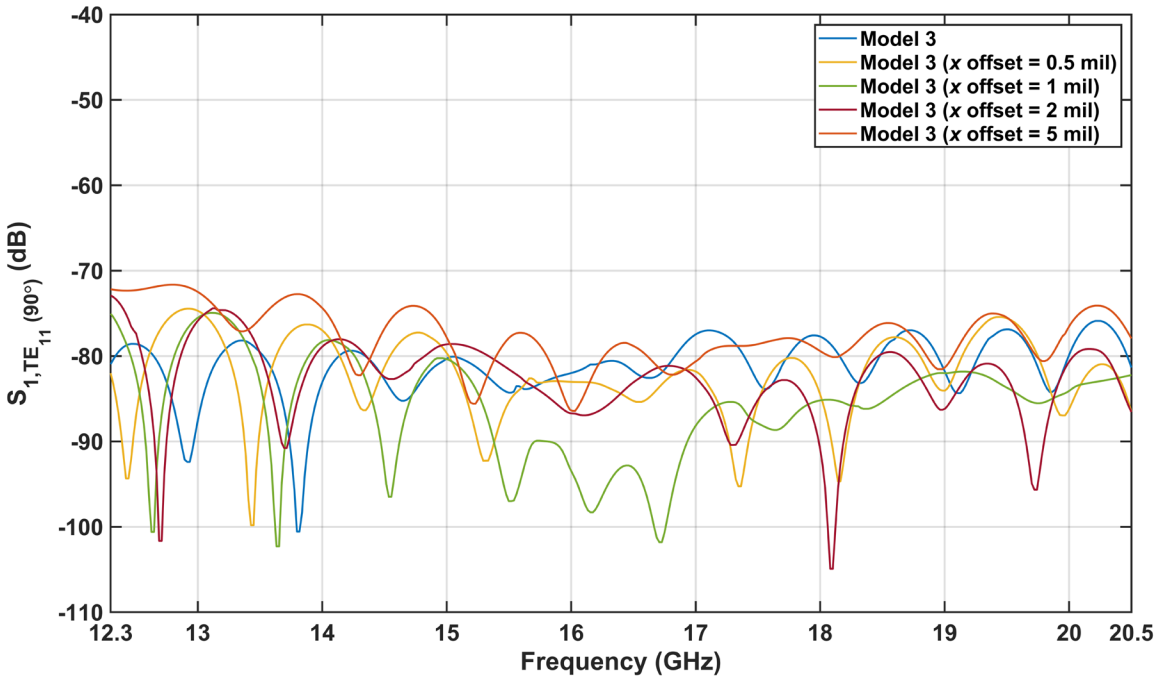

Figure 24. Cross-pol vs. Tolerance (offsets in x-axis)

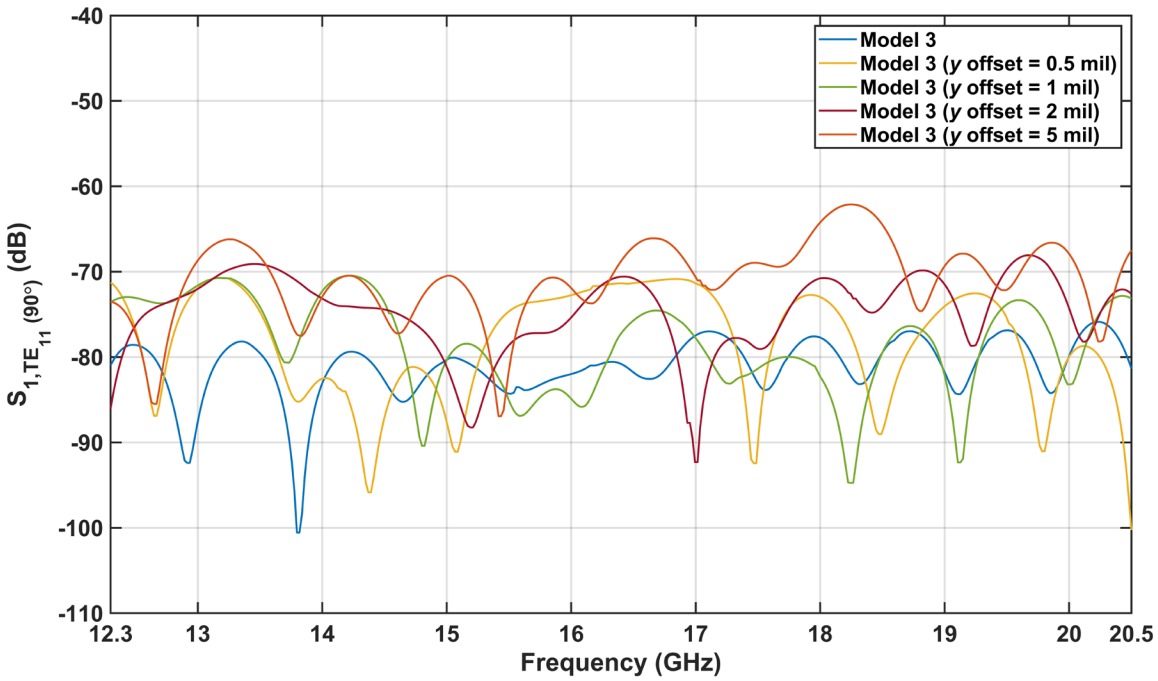

Figure 25. Cross-pol vs. Tolerance (offsets in y-axis)

Lastly, the simulation did predict higher coupling to the TM01 and TE21 as the tolerance offset is increased. The coupling to TM01 is more pronounced in the y-axis offset (max of -40 dB at 5 mil offset), while coupling to TE21 is comparable for x- and y-axis offsets (max of -40 dB at 5 mil offset). These results, however, are not expected to be an issue for the application of this component.

Overall, degradation due to the tolerances simulated was minimal. While a 1-2 mil tolerance would be desired for manufacturing, a 5 mil tolerance would be acceptable.

Non-linear transitions

Simulations were performed on non-linear transitions with $\sin^n$ profiles defined along the 8 edges of a transition. The results are omitted here for brevity; however, in summary these transitions did not perform nearly as well as the Model 3 linear transition over the full frequency band.

Fabrication

Electroforming techniques have traditionally been used to create these transition geometries. This process has machined a metal (Aluminum) mandrel on which electrodeposition occurs, followed by a parting (dissolution) of the mandrel. Machined parts can achieve an RMS roughness of 0.2 – 0.3 um, and an electroformed part should have this roughness, or somewhat better. Relative to skin depth in this frequency range, the smooth surface roughness minimizes the added RF loss.

Other modern techniques could be explored for building these transitions, for instance:

- Electric discharge machining (EDM)
- Direct 3D metal printing
- 3D printed mandrels for electroforming

- 3D printed structure with perforations, followed by electroplating

It is expected that the surface roughness is significantly higher when using 3D-printing, however, this will likely continue to improve with advances in technology. For the waveguide transition in this particular application, a small amount of extra RF loss due to roughness could be corrected for in the Vector Network Analyzer calibration. The geometry of these rectangular to circular transitions may be amenable to 3D-printing, as the shape changes gradually and without sharp overhangs.

Summary

As these electromagnetic simulations predict, not all linear waveguide transitions are created equal. Performing a Loft in Inventor using the default settings creates a transition with a cross-section composed of 4 arcs. This geometry appears to be inferior in simulation compared to the other transitions having 4 straight edges and arcs in the corners of the cross-sections.

The “Model 3” geometry definition described above achieves the best simulation results of those considered here for a given length and is easy to define and model. This design at a length of 12 cm is the recommended transition for the purposes of ngVLA Band 3 testing of feed horns and OMTs. Better than 35 dB return loss, less than 0.03 dB insertion loss, and more than 80 dB cross-pol isolation are simulated. The contribution of this transition to the uncalibrated response in a Vector Network Analyzer (VNA) test setup will be minimal.

The introduction of manufacturing tolerances in the simulation creates asymmetry in the model. Performance deviation from the original simulation only slightly with tolerances of 1-2 mil. With a tolerance of 5 mil, the performance degradation is more apparent, but still acceptable.

Acknowledgements

Thank you to Cam Bryant for discussion and modeling a transition in Inventor that approximates the CHAMP 3D generated model.